

# THE PHYSICAL REVIEW

*A journal of experimental and theoretical physics established by E. L. Nichols in 1893*

SECOND SERIES, VOL. 74, No. 5

SEPTEMBER 1, 1948

## Photographic Plates for Use in Nuclear Physics†

J. H. WEBB

*Research Laboratories, Eastman Kodak Company, Rochester, New York*

(Received April 13, 1948)

The registration of charged particles by the photographic emulsion is considered from the standpoint of their space rate of energy loss on passage through matter. On the basis of the highest-energy particles that can be recorded as recognizable tracks, an energy-loss value of 0.013 Mev per centimeter of air path is taken as an approximate threshold sensitivity value of the best present-day nuclear-particle emulsions. This energy-loss value corresponds to alpha-particles of energy  $>400$  Mev, deuterons of 100 Mev, protons of 50 Mev, and electrons of 20 kev. Some evidence is cited to show that these limiting energy values are in accord with experience.

Range-energy curves for alpha-particles, protons, deuterons, and mesons in high silver halide concentration emulsions are given, based on constant stopping-power values of the emulsion. A relative stopping-power value of 1800 is used for alpha-particles, and a value of 2000 is used for protons, deuterons, and mesons.

Data on the composition, physical characteristics, and sensitivity, and also recommended uses of some of the commercially available nuclear-particle emulsions are presented.

A theoretical calculation of the stopping power of the photographic emulsion relative to that of air is given. Curves of stopping power *versus* energy for alpha-particles and protons in a high silver halide content emulsion are calculated and compared with published experimental values.

Grain density and its variation in the recorded tracks of nuclear particles in the photographic emulsion are discussed. It is pointed out that the grain density for low-energy particles approaches a maximum value determined by the grain population of the unexposed emulsion. A qualitative discussion is given to show why grain spacing varies with particles of differing ionizing power.

Finally, the mechanism of latent-image formation is considered from the standpoint of ion-pair production in the grain. Using the energy-loss value of 0.013 Mev per centimeter as a threshold limit and a value of 7.6 ev for the energy required to produce an ion pair in silver bromide, it is shown that about 150 ion pairs must be produced in a single grain to form the latent image.

IN 1896 Becquerel discovered that uranium salts emit radiations capable of blackening a photographic plate. In the early work in radioactivity, the photographic plate was, in fact, about the only means of detecting the radiations from these newly discovered materials. Later, however, as more quantitative work on radiations associated with radioactivity came to be done, other methods of measurement came into general use.

In 1911 Wilson introduced the cloud chamber

which was the first instrument actually to show the paths of individual nuclear particles. It was at about this same time that the photographic emulsion was first shown to be capable of registering the paths of nuclear particles. In 1910 Kinoshita<sup>1</sup> demonstrated that photographic grains were affected by alpha-particles and, furthermore, that the impact of a single alpha-particle was probably sufficient to produce a developable latent image in a grain. In 1912 Reinganum<sup>2</sup> showed that the path of an alpha-

† Communication No. 1182 from the Kodak Research Laboratories.

<sup>1</sup> S. Kinoshita, Proc. Roy. Soc. (London) **83A**, 432 (1910).

<sup>2</sup> M. Reinganum, Physik. Zeits. **10**, 1276 (1911).

particle in an emulsion could be registered as a line of developable grains. Since this discovery, many workers have made use of the photographic plate for the registration and study of single nuclear events. Among the pioneers in this field the names of Blau and Wambacher and Wilkins are to be especially pointed out. For a summary of all work along these lines up to 1941 the reader is referred to the excellent review by Shapiro.<sup>3</sup>

The photographic plate resembles very closely the cloud chamber in its ability to record individual nuclear events, but it does not give the fine distinction between tracks of different types of particles nor the possibility of recording the bending of particles in a magnetic field as does the cloud-chamber technique. However, because of its higher stopping power, continuous sensitivity, and simplicity, the photographic plate offers certain advantages not possessed by the cloud chamber. Particles that can be observed in the cloud chamber are alpha-particles, protons, deuterons, positrons, electrons, and mesotrons. It is highly desirable that the photographic plate should be developed to a point where it will record all these particles over wide ranges of energy. Obviously, a photographic plate that could achieve this goal, together with its higher stopping power and permanent record, would be an exceedingly important tool for the nuclear physicist.

It is the purpose of the present paper to show how far the photographic plate has been developed in this direction, what is available now,

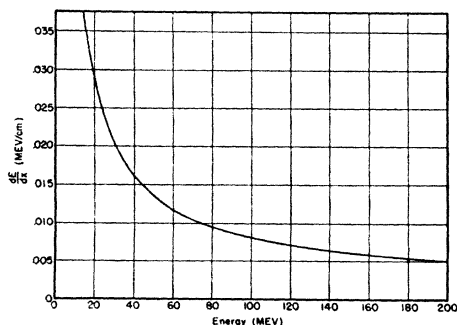


FIG. 1. Theoretical curve of space rate of energy loss for protons in air according to Eq. (1). From calculations by J. H. Smith, Phys. Rev. 71, 32 (1947).

<sup>3</sup> M. M. Shapiro, Rev. Mod. Phys. 13, 58 (1941).

and what are the prospects for the future. A general outline is given of the mechanism by which charged particles affect the photographic plate. The composition and structure of present-day nuclear-track plates are discussed and a method of calculating the stopping power of an emulsion of known composition is presented. The question of grain spacing and the factors upon which it depends are considered, and finally some aspects of latent-image formation are discussed, with particular reference to the number of ion pairs required to produce developability in a single grain. In discussing all these topics, an attempt is made to cite experimental evidence to show that the conclusions reached are in line with practical experience. This paper does not purport to present novel and unusual experimental results. (While the present paper was in course of preparation, two excellent papers on this same general subject have appeared by Demers<sup>4</sup> and by Lattes, Fowler, and Cür.<sup>5</sup> These two papers present considerably more experimental data on the nuclear-particle plates than are given here and are highly recommended to the reader. Also, the beautifully illustrated book just published by Powell and Occhialini<sup>6</sup> is recommended to the worker in this field.) Rather, the subjects treated and the experimental data presented are intended as a guide to an understanding of the action of the photographic plate as a tool in nuclear research.

#### SPACE RATE OF ENERGY-LOSS AND RANGE-ENERGY CURVES FOR CHARGED PARTICLES IN AIR

In Fig. 1 is shown a curve of energy loss per centimeter of path on passage of a proton through air. This curve gives the loss of energy in Mev per centimeter as a function of the energy of the proton in Mev and was plotted from the theoretical data computed by J. H. Smith,<sup>7</sup> using the following equation<sup>8-10</sup> for the average energy

<sup>4</sup> P. Demers, Can. J. Research 25, 223 (1947).

<sup>5</sup> C. M. Lattes, P. H. Fowler, and P. Cür, Proc. Phys. Soc. (London) 59, 883 (1947).

<sup>6</sup> C. F. Powell, and G. P. S. Occhialini, *Nuclear Physics in Photographs* (Oxford University Press, London, 1947).

<sup>7</sup> J. H. Smith, Phys. Rev. 71, 32 (1947).

<sup>8</sup> M. S. Livingston, and H. Bethe, Rev. Mod. Phys. 9, 263 (1937).

<sup>9</sup> B. Rossi, and K. Greisen, Rev. Mod. Phys. 13, 249 (1941).

<sup>10</sup> J. Wheeler, and R. Ladenberg, Phys. Rev. 60, 761 (1941).

loss per unit thickness of stopping material:

$$(dE/dx) = -[4\pi(ze)^2N/mv^2] \cdot \{Z[\ln(2mv^2/I) - \ln(1 - \beta^2) - \beta^2] - C_K\}, \quad (1)$$

in which

- $ze$  = charge of the incident particle;
- $v$  = velocity of the incident particle;
- $N$  = number of atoms per cubic centimeter of stopping material;
- $Z$  = atomic number of stopping atoms;
- $I$  = average ionization potential of stopping material;
- $m$  = electron mass;
- $\beta = v/c$ ,  $c$  the velocity of light;
- $C_K$  = a corrective term which must be applied in case  $v$  is comparable with the velocity of the  $K$  electron of the stopping material but large compared with that of all others.

The main portion of the energy loss, suffered by charged particles traversing matter, goes into production of ions through the interaction of the bombarding particles with the electrons of the stopping material. The loss of energy varies directly with the square of the charge,  $(ze)^2$ , of the incident particle, inversely as the square of the velocity,  $v$ , of the incident particle, and directly with the number of electrons per cubic centimeter,  $(NZ)$ , of the stopping material. The quantity

$$B = Z \ln(2mv^2/I) \quad (2)$$

has been designated as the stopping number of an atom of the stopping material, and the ratio of  $B$  for a given material to the  $B_0$  for air as the relative stopping power of the atom of that material; thus,

$$s_a = B/B_0. \quad (3)$$

The range-energy curve for a charged particle in air can be obtained from the rate of energy loss curve from the integral,

$$R = \int_0^E [dE/(dE/dx)]. \quad (4)$$

The range-energy curve for protons in air, as computed by J. H. Smith,<sup>7</sup> is shown in Fig. 2. From the curves for energy loss and range for a

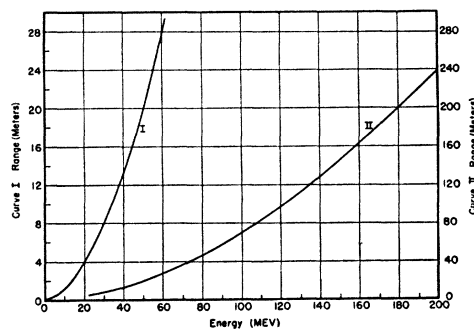


FIG. 2. Theoretical range-energy curves for protons in air according to Eq. (4). From calculations by J. H. Smith, Phys. Rev. 71, 32 (1947).

given type of particle (characterized by a particular value of charge  $(ze)$  and mass  $(M)$ ) it is possible to determine the energy-loss and range curves of other particles of different  $z$  and  $M$  values by means of relations (5) and (6) given below for alpha-particles and protons as examples. Thus, if an alpha-particle and a proton are assumed to have the same velocities, then

$$(dE/dx)_{\alpha, v} = (z_{\alpha}/z_H)^2 (dE/dx)_{H, v}, \quad (5)$$

$$R_{\alpha}(v) = (z_H/z_{\alpha})^2 (M_{\alpha}/M_H) R_H(v);$$

or, since particles having the same velocities have energies in proportion to their mass values, the relations (5) can be expressed in terms of energies of the particles:

$$(dE/dx)_{\alpha, E} = (z_{\alpha}/z_H)^2 (dE/dx)_H \left( \frac{M_H}{M_{\alpha}} E \right) \quad (6)$$

$$R_{\alpha}(E) = (z_H/z_{\alpha})^2 (M_{\alpha}/M_H) R_H((M_H/M_{\alpha})E).$$

The relations (5) and (6) are very convenient for transposing energy-loss and range values from one particle to another of different  $z$  and  $M$  values.

In Fig. 3, energy-loss curves in Mev per centimeter of air path for alpha-particles, deuterons, protons, mesons (mass 0.1 of proton), and electrons are shown to the same scale. The proton curve is the same as that shown in Fig. 1, and is therefore accurate with respect to relativity corrections, etc., to the full 400-Mev value shown. The curves for the alpha-particles, deuterons, and mesons were derived from the proton curve by means of the relation (6) and, though not so accurate as the proton curve, are adequate

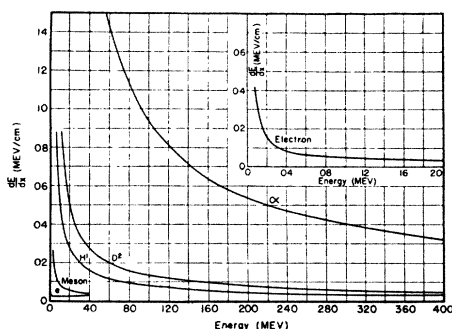


FIG. 3. Theoretical curves of space rate of energy loss for  $\alpha$ -particles, deuterons, protons, mesons, and electrons in air.

for the purpose here. The energy-loss curve for the electron is shown on an enlarged scale in the upper right section of Fig. 3.

The reason for showing the energy-loss curves is that they bear a close relationship to the mechanism by which high-velocity charged particles act on a photographic grain to produce developability and therefore will be of material aid in discussing this problem.

#### PRESENT LIMIT OF PHOTOGRAPHIC SENSITIVITY FOR CHARGED PARTICLES

The threshold sensitivity of nuclear-track plates can best be designated in terms of the lowest rate of energy loss for which a particle will register as a just recognizable line of grains. With the best modern nuclear-track plates, there is evidence to indicate that this limit is reached for deuterons of around 100-Mev and protons of around 50-Mev energy. Thus, on an Eastman NTB plate exposed to the 190-Mev deuteron beam of the University of California cyclotron, individual tracks have been followed in the microscope over path lengths from their stopping end of the order of 2 cm.\* Assuming a stopping power of 2000 for the emulsion, this would give an equivalent air path of 40 meters, corresponding to that of a 100-Mev deuteron. The high-velocity end of such a residual track consists of widely and irregularly spaced grains. Therefore, it must be supposed that only those grains of highest sensitivity and those most favorably hit by the charged particles are made developable under these conditions.

\* From visual observations through the microscope made in the Kodak Research Laboratories.

Direct evidence on the sensitivity of the nuclear-track plates is given by the pictures shown in Fig. 4. The upper photograph shows an Eastman NTB plate that was exposed edgewise to the 190-Mev deuteron beam in the University of California cyclotron. The deuterons hit the glass plate, on which the emulsion is mounted, edge on, and traveled mostly in the glass. As they emerged through the surface of the glass, they produced tracks in the emulsion that are characteristic of their energy at that point. The darker section at the bottom corresponds to the more intense part of the beam. It can be seen that the darkening of the plate is faint over most of the 6.9-cm range of the particles, but increases steeply near the end of the path, in accordance with the Bragg curve of ionization. It is interesting to note that while the range of the 190-Mev deuterons in glass is 6.9 cm, the range for the same energy deuterons in the photographic emulsion would be 6.4 cm, based on a relative stopping power of 2000. Thus, the stopping power of the glass and that of the photographic emulsion are not very different.

In order to determine how the varying energy deuterons register as tracks on the NTB plate, photomicrographs were made of sample tracks on a plate that had received a somewhat lighter exposure than the above plate, at points 0, 0.5, 1, 2, 4, and 6 cm from the end of their range. These tracks are shown in the lower part of Fig. 4. Only the parallel tracks are to be considered, because the diagonal tracks result from deflected or secondary particles of reduced velocity. It can be seen that dense tracks are obtained at the 0.0- and 0.5-cm positions ( $\sim 45$  Mev), less dense tracks at the 1-cm position ( $\sim 64$  Mev), and still less dense, but recognizable, tracks at the 2-cm position ( $\sim 95$  Mev). At the 4-cm position ( $\sim 138$  Mev), the tracks have become somewhat tenuous and at the 6-cm position ( $\sim 185$  Mev) are composed of widely spaced grains. From these pictures it is evident that there is no sharp cutoff in sensitivity with increasing energy. However, when the tracks on these plates are viewed in the microscope it is apparent that the quality of the tracks have deteriorated considerably for energies above 100 Mev.

From the deuteron curve of Fig. 3 it can be seen that a 100-Mev energy corresponds to an

energy-loss value in air of 0.013 Mev per centimeter. Assuming that this is the threshold energy-loss value for which enough grains will respond to give a recognizable track, the following limiting energy values for other particles that will give tracks of comparable quality may be set down:

Deuteron	100 Mev
Proton	50 Mev
$\alpha$ -particle	>400 Mev
Meson (200 Me)	5 Mev
Electron	0.022 Mev

It is of interest to point out that Eastman NTB plates exposed to the 380-Mev alpha-particles of the University of California cyclotron recorded particles of this energy. Though the whole track length ( $\sim 3.2$  cm) corresponding to this energy could not be recorded in the thin emulsion layer, nevertheless it was observed that the beginnings of the tracks of many alpha-particles of this energy were recorded. Tracks of protons of high energy have been recorded on

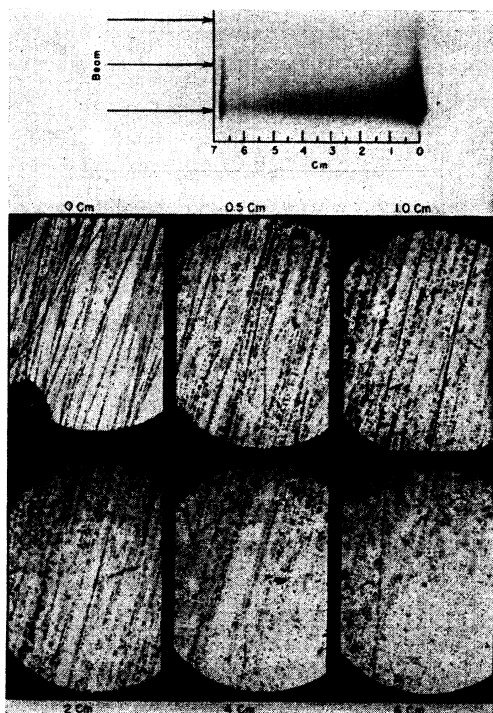


FIG. 4. Photographic effect of 190-Mev deuterons on nuclear-track plates. Upper picture = over-all density due to deuterons as they are slowed. Lower picture = photomicrographs of tracks of deuterons at various distances from the stopping end.

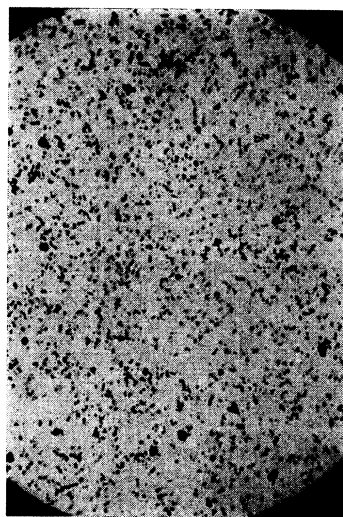


FIG. 5. Photomicrograph of Eastman NTB plate, exposed to 30-kv electrons, showing tracks of 4-5 grain length.

Ilford halftone plates by H. Wambacher.<sup>11</sup> One of these recorded tracks had a path length of 2 cm in the emulsion. If a value of 1300 is taken for the stopping power relative to air for the emulsion used, this would give an air path of 26 meters, corresponding to an energy of 57 Mev. Also, a number of workers<sup>12-17</sup> have given experimental results on meson tracks in emulsions. Lattes, Muirhead, Occhialini, and Powell<sup>12</sup> point out that on the basis of sensitivity estimates mesons of energy higher than 5 Mev probably cannot be detected with Ilford C2 plates. In a later paper by Lattes, Occhialini, and Powell,<sup>16</sup> meson tracks of varying residual ranges were analyzed. The energy can be estimated from the range, if a value for the mass is assumed for the meson. With an assumed mass of 200 electron masses, the tracks corresponded to 4.1-Mev mesons. These results are merely cited as evidence that particles having energies between zero and the limits set above are capable of recording as recognizable tracks in the nuclear-particle plates.

<sup>11</sup> H. Wambacher, Sitz. Akad. Wiss. in Wien, Math.-Naturwiss. Klasse Abteilung IIa, 149, Heft 3-4, 157 (1940).

<sup>12</sup> C. M. G. Lattes, H. Muirhead, G. P. S. Occhialini, and C. F. Powell, Nature 159, 694 (1947).

<sup>13</sup> D. M. Bose, and B. Choudhuri, Nature 148, 259 (1941).

<sup>14</sup> D. H. Perkins, Nature 159, 126 (1947).

<sup>15</sup> G. P. S. Occhialini, and C. F. Powell, Nature 159, 186 (1947).

<sup>16</sup> C. M. G. Lattes, G. P. S. Occhialini, and C. F. Powell, Nature 160, 453 (1947).

<sup>17</sup> C. M. G. Lattes, G. P. S. Occhialini, and C. F. Powell, Nature 160, 486 (1947).

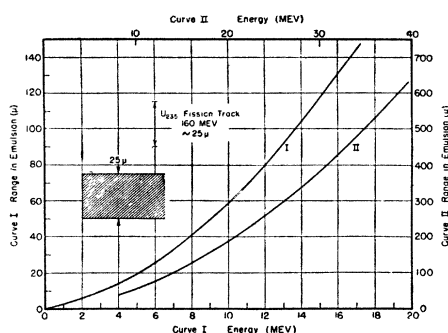


FIG. 6. Range-energy curve for  $\alpha$ -particles in nuclear-track plate of high AgBr concentration. Drawn for constant stopping power of 1800.

Until very recently, indisputable tracks of electrons in emulsions had not been observed. However, in a recent paper Demers<sup>4</sup> stated that with very sensitive emulsions of his own manufacture he had observed faint complicated tracks of a few grains' length which he attributed to electrons. Subsequent to Demers's paper, tracks of electrons were obtained by members of the Eastman Kodak Research Laboratory<sup>18</sup> at Harrow, England, with their high-sensitivity proton plates. Electron tracks have now been observed on the Eastman NTB plates and an illustration is given in Fig. 5. This plate was exposed to 30-kv electrons in the RCA electron microscope, with the electron beam perpendicular to the plate. As can be seen, the tracks are short and wavy and consist of only a few grains each. From the energy-loss curve for electrons shown in Fig. 3, the limiting energy electron that will make a grain developable is about 0.022 Mev. An electron of this energy would have a residual range in air of approximately 0.7 cm. If a stopping power of 2000 is assumed for the emulsion, this would correspond to a path length in the emulsion of  $3.5\mu$ . Therefore, only a few grains (three to four) at the very end of the electron path could be made developable. Here, again, the action of the electrons on the emulsion grains appears to be in line with what is to be expected on the basis of energy-loss data.

From what has been said it may be concluded that in the nuclear emulsions being made today a moderate fraction of the grains will be affected by particles whose energy-loss value is as low as

<sup>18</sup> R. W. Berriman, *Nature* **161**, 432 (1948).

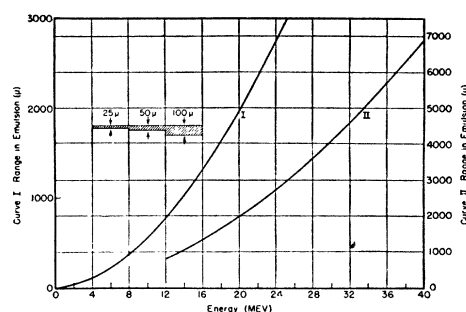


FIG. 7. Range-energy curve for protons on nuclear-track plates of high AgBr concentration. Drawn for constant stopping power of 2000.

0.013 Mev per centimeter in air. This limit, while somewhat arbitrary, is based on the criterion that the emulsion contains a certain fraction of grains with sufficiently high sensitivity that a particle of this energy-loss value will register as a detectable line of grains.

It is interesting to compare the figure of 0.013 Mev per centimeter with the minimum energy-loss values of the curves of Fig. 3 in order to see how far present-day emulsions are from the point of registering the highest-energy particles. It may be pointed out that all the energy-loss curves of Fig. 3 go through a broad flat minimum, which is closely the same for all types of particles, i.e., about 0.0022 Mev per centimeter. Thus, it can be seen that an emulsion with a threshold sensitivity of some five to six times lower value would be required in order to register particles of any energy value whatever. Even though this ultimate goal may be unattainable, an inspection of the curves of Fig. 3 will show that even slight improvement in the threshold sensitivity value will tend to push upward disproportionately the energy value of particles that can be registered. Considering the short time that serious development work on the nuclear-track plates has been in progress, it does not appear impossible that the sensitivity might be pushed to a point corresponding to an energy-loss value of 0.0022 Mev per centimeter.

#### RANGE-ENERGY CURVES FOR CHARGED PARTICLES IN A PHOTOGRAPHIC EMULSION

To illustrate the range-energy relationship for nuclear-track plates of high silver bromide concentration, curves showing range in microns ( $\mu$ ) versus energy in Mev are given for alpha-particles

and protons, respectively, in Figs. 6 and 7. The curve for alpha-particles shown in Fig. 6 was constructed assuming a constant stopping power of emulsion relative to that of air of 1800. This figure was selected on the basis of the general average of results obtained in tests of Eastman NTA and NTB emulsions exposed to alpha-particles of energy below 9 Mev, obtained from natural radioactive materials such as thorium, polonium, and uranium. Every batch of Eastman NTA plates is given a standard test to polonium alpha-particles (5.3 Mev) and these tests consistently give a range value between 21 and 22 $\mu$  in close agreement with the stopping power value of 1800.

Data published by Tsien San-Tsiang, Chastel, Faraggi, and Vigneron<sup>19</sup> for alpha-particles on Ilford new halftone concentrated plates are given below:

	<i>E</i> (Mev)	Range in emulsion ( $\mu$ )	Stopping power relative to air
ThC'	8.77	46.1	1860
ThC	6.05	26.2	1810
Po	5.29	21.4	1790
UI	4.71	18.8	1710
UII	4.15	15.6	1700

These values indicate the falling off of stopping power to be expected at low energies. Later in this paper, the question of stopping power of the emulsion will be discussed more fully and a method will be given for calculating this quantity, using the stopping power of the constituent atoms of the emulsion and the composition of the emulsion.

For energies above 10 Mev there have been so few range-energy measurements made for alpha-particles in emulsions that a curve based on experience cannot be drawn for this region. Therefore, until additional measurements of range-energy values are made for energies above 10 Mev, the curve for this region of Fig. 6 must be considered as an approximation.

The straight vertical arrow in Fig. 6, marked U<sup>235</sup> fission track, is representative of the range obtained by several workers<sup>20-22</sup> who used photo-

<sup>19</sup> Tsien San-Tsiang, R. Chastel, H. Faraggi, and L. Vigneron, *Comptes rendus* **223**, 571 (1946).

<sup>20</sup> P. Demers, *Phys. Rev.* **70**, 974 (1946).

<sup>21</sup> K. Lark-Horowitz, and W. A. Miller, *Phys. Rev.* **59**, 941 (1941).

<sup>22</sup> L. L. Green, and D. L. Livesey, *Nature* **158**, 272 (1946).

graphic emulsions for recording fission tracks. The range (25 $\mu$ ) indicated by the arrow corresponds to the full length of the track for both fragments. One of these tracks, obtained on an Eastman NTC emulsion, is shown in Fig. 19, and it may be noted that the grain density is greatest in the middle portion. The high charge on the fragments immediately after fission causes the heavy initial ionization in spite of the high velocity of the particle. As the fission fragments lose velocity, it might be expected that the ionization would increase. However, the loss of charge of the fragment more than overbalances the effect of reduced velocity, and the net result is a reduction in ionization, as indicated by the lower grain density of the track toward its extremities. It is interesting to estimate the average effective charge of a fission fragment from the observed range of the fragments for U fission, using the relation (6),

$$R_{\text{fiss}}(E) = (z_H/z_f)^2 (M_f/M_H) R_H((M_H/M_f) \cdot E).$$

Inserting the relative-mass values of fission fragment to proton as 117 and an estimated average value of the charge on the fission fragment of 10, we obtain, for the 160-Mev energy of the combined fission fragments,

$$R_f(160) = (1/100)117R_H(1.36) = 4.68 \text{ cm air,}$$

or a range in the emulsion, using a stopping power of 1800,

$$R_f = 26\mu.$$

Thus, when one assumes an average charge value of 10 for the fission fragments, a range value in close agreement with experiment is found.

Also, a cross section of an emulsion 25 $\mu$  thick is shown to scale in Fig. 6, for comparison with the track lengths. It can be seen that a 25 $\mu$  emulsion is thick enough to register alpha-particles of moderate energy value without too much chance of the tracks running out of the emulsion. However, for energy values above 15 Mev, thicker emulsions up to 50 or even 100 $\mu$  are desirable. In Fig. 7 is given a range-energy curve for protons up to energies of 40 Mev. The curve is drawn for a constant value of stopping power of the emulsion relative to air of 2000 instead of 1800, as used for the alpha-particle curve. This value was chosen from the results of

tests on Eastman NTB emulsions exposed to protons of energy below 10 Mev. In this connection, Eastman NTB emulsions are regularly tested with 7.0-Mev protons from the University of Rochester cyclotron, and the range values obtained in these tests have averaged  $300\mu$ , which, compared with the 60-cm air path for these particles, corresponds closely to a stopping power of 2000. Actually, the stopping power of the photographic emulsion is not a constant value independent of energy of the particle, but increases with energy rather sharply at low energies of the particle and flattens out into a gradually rising curve for higher energies, as shown in Fig. 9. As can be seen from this figure, the plateau region of the stopping-power curve is reached at considerably lower energy values for protons than for alpha-particles and this is in line with the higher stopping-power value of 2000 used in Fig. 7. Owing to the lack of experimental data on the stopping power of the range-energy curve of nuclear plates for energies above 10 Mev and also because of the variation of stopping power at very low energies, the range-energy curves of Figs. 6 and 7 are to be regarded merely as fairly reliable guides to the range-energy relationship.

In Fig. 7, cross sections of emulsions of thicknesses 25, 50, and  $100\mu$  are shown for purposes of comparison with the proton tracks of varying energy. Commercial emulsions are now available in thicknesses up to  $100\mu$ . For protons of energy above 10 Mev, the  $100\mu$  emulsion is required in order to insure that a good fraction of the tracks will fall within the angle tolerance limits afforded by this thickness of emulsion.

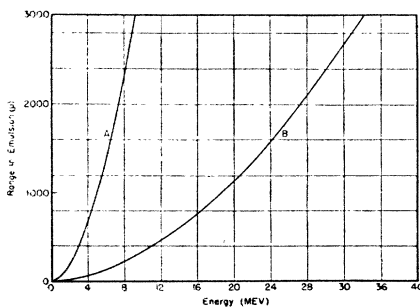


FIG. 8. Range-energy curves for (A) meson (0.1 mass of proton) and (B) deuteron on nuclear-track plates of high AgBr concentration. Drawn for constant stopping power of 2000.

For completeness, range-energy curves for mesons and deuterons in an emulsion are shown in Fig. 8. Both curves were drawn for a constant stopping power of 2000, and the mass assumed for the meson is one-tenth of the proton mass.

According to the foregoing discussion, it is obvious that for the registration of high-energy particles emulsions of much greater thickness than  $100\mu$ , in fact, up to several millimeters, would be desirable. Unfortunately, there are several obstacles to the use of emulsions of such great thickness. Coatings of a gelatin emulsion greater than  $100\mu$  are exceedingly difficult to deal with mechanically. A  $100\mu$  coating on film will cause it to curl and twist to an extent that makes it almost impossible to handle. If placed on glass plates, the gelatin will peel off because the forces exerted are sufficient to fracture the glass surface on which it is mounted. In addition to these troubles, there are formidable difficulties in processing thick emulsions. Both the development and fixing procedures depend upon a process of diffusion of the chemicals into the emulsion layer and of reaction products out of the layer. As the chemical agents become exhausted within the layer, replenishment of fresh chemical is needed, and therefore a process of exchange diffusion is required if the image is to be fully developed and fixed. Even in emulsions of  $100\mu$  thickness, development and fixing are carried out with difficulty, and sometimes there is evidence of variation of response at varying depths of the layer because of the non-uniform processing conditions.

Finally, it should be pointed out that the thickness of emulsion that can be examined with the microscope is limited by the working distance of the objective used. With an oil-immersion objective of 1.8-mm focal length and 97 power, the maximum working distance in the emulsion, without a cover glass, is 300 microns.

#### COMMERCIAL NUCLEAR-RESEARCH EMULSIONS

Nuclear-research emulsions of the type discussed here are manufactured by the Ilford Company and Kodak, Ltd., in England and by the Eastman Kodak Company in America.

The Ilford research laboratory issues a pamphlet describing its emulsions for recording particle tracks and giving photographic charac-



TABLE I. Eastman nuclear plates.

	Type NTA	Type NTB*	Type NTC
Sensitivity	To nuclear particles Alpha-particles to 200 Mev, Protons to 20 Mev, Deuterons to 20 Mev	Alpha-particles to 400 Mev, Protons to 50 Mev, Deuterons to 100 Mev, Mesons to 5 Mev	Nuclear-fission fragments of high ionizing power only
	To light, gamma rays, and beta rays	low	moderate
	To show energy-loss rate by grain spacing	2 minutes at 68°F in D-19	very low
Development	To render tracks very clear for counting	2 minutes at 68°F in D-8** diluted 2:1	special instructions
Recommended fixation	F-5 or 30 percent hypo	30 percent hypo	special instructions
Emulsion thickness	25 $\mu$ regular (to 100 $\mu$ on request)	50 $\mu$ and 100 $\mu$ (process 100 $\mu$ by special instructions)	25 $\mu$
Silver bromide content—percent weight of dry emulsion	83 percent	83 percent	65 percent
Grain size (approx.)	0.2–0.4 $\mu$ diam.	0.2–0.3 $\mu$ diam.	0.1–0.4 $\mu$ diam.

\* Recommended for all higher-energy particles of low ionizing power.

\*\* To obtain best response to low ionizing particles such as mesons and electrons the following alternate development is recommended: Soak in water for five minutes; develop in D-19 diluted 1 : 3 for 22 min. at 68°F. Fix in 30 percent hypo for twice the time to clear.

teristics and composition. In the pamphlet accompanying the plates, the Ilford laboratory gives the following list and description of its nuclear-particle emulsions:

“Type B-2—Fine grain and the most sensitive emulsion of the series, giving good tracks of  $\alpha$ -particles and 2–4 Mev protons.

“Type C-2—Finer grain than B-2, giving more clearly defined  $\alpha$ -particle and proton tracks. Specially made for giving measurable proton tracks.

“Type E-1—Of very slightly finer grain than C-2, giving improved  $\alpha$ -particle records, suitable for accurate measurement of range. The tracks formed by protons are poor, thus distinguishing clearly between these and  $\alpha$ -particles.

“Type D-1—Of finer grain than E-1.  $\alpha$ -particle tracks poor, protons do not record but good fission tracks are obtained.

“The following may perhaps be regarded as obsolescent but are still produced to special order.

“Type B-1—Has grain characteristics similar to B-2 but sensitivity similar to C-2. B-2 and C-2 are believed to be preferable alternatives.

“Type C-1—Similar to E-1 but of slightly coarser grain and slightly greater sensitivity.

Gives inferior discrimination between  $\alpha$ -particles and protons of low energy.

“Standard emulsion thickness are 50 $\mu$  and 100 $\mu$ . All emulsions, except C-1 and D-1 may be supplied loaded with lithium, boron, or beryllium, or with a lower concentration of silver in the gelatin medium. . . .

“All these emulsions, in standard form, have the same chemical composition. This is approximately as follows, in grams of each element per cubic centimeter of emulsion, under normal atmospheric conditions: Ag—1.87; H—0.056; Br—1.36; O—0.24; I—0.053; S—0.014; C—0.33; N—0.083; Ca, P, Cr, Si, Na—traces.”

The Ilford Company also publishes tables of range-energy values, based on actual measurement, for the energy range 0–10 Mev and extrapolated range-energy values for the energy range 10–35 Mev, for both alpha-particles and protons.

The range-energy values published by Ilford do not differ greatly from the values given in Figs. 6 and 7 for alpha-particles and protons below 10-Mev energy. However, there are some differences above 10 Mev. This is because the curves of Figs. 6 and 7 were drawn using a constant stopping power for all energy values. In the

TABLE II. Composition of Eastman nuclear-track plates.

Element	NTA and NTB		NTC	
	Percent	Atomic ratio	Percent	Atomic ratio
Ag	47.1	1.0	38.0	1.0
I	1.49	0.027	1.24	0.027
Br	33.9	0.97	27.4	0.979
C	8.47	1.62	16.2	3.83
H	1.17	2.68	2.25	6.38
N	3.06	0.50	6.84	1.17
O	4.80	0.69	9.09	1.62
Relative humidity, percent	Moisture content—percent weight of dry emulsion			
50	2.2		4.5	
70	4.0		8.0	

next section, the matter of stopping power is treated more in detail and curves of range energy, using varying stopping power, are given.

Kodak, Ltd. in England has very recently started to make a nuclear-particle plate designated as NTP-2A. It is a high-sensitivity plate especially recommended for registering high-velocity particles of low ionizing power. In its experimental stage, it was the first plate to register well-recognizable electron tracks. These plates are now marketed as a standard item in size 1"×3" and 50 $\mu$  thickness. The sensitivity, stopping power, and physical characteristics are closely the same as those of the NTB plate made by the Eastman Kodak Company in America and described in the following paragraphs.

At present, the Eastman Kodak Company is marketing three general types of nuclear-track plates classified under the headings: NTA, NTB, and NTC. The general properties and recommended processing conditions for these emulsions are presented in Table I.

Examples of tracks of different nuclear particles registered on these plates are shown in Figs. 16-19. It should be mentioned that the NTA and NTB plates can be supplied impregnated with the elements, boron, lithium, and beryllium, the amount of impregnating material being specified in milligrams per square centimeter for each batch of plates. Specific instructions for handling and processing these plates are supplied by the manufacturer with each batch of plates.

For certain purposes, it is desirable for the nuclear physicist to have an accurate knowledge

of the composition of the photographic plate that he uses. Accordingly, the following figures on the composition of Eastman emulsions are given. All emulsions are essentially mixtures of gelatin and silver bromide. The composition of the gelatin expressed in weight percent is as follows:

Gelatin composition, percent	
Carbon	50.0
Hydrogen	6.7
Nitrogen	18.0
Oxygen	25.0

The nuclear-particle plates have a relatively higher percentage of silver bromide than the normal photographic emulsion. The Eastman NTA and NTB emulsions have the same composition, containing about 83 percent silver halide and 17 percent gelatin. The NTC plate contains about 65 percent silver halide and 35 percent gelatin. In Table II the composition of the Eastman NTA, NTB, and NTC plates is given in terms of percent weight and in terms of atomic ratios, as determined from chemical analysis of the dry emulsions. The atomic composition values must be corrected for moisture content according to the figures in the lower part of Table II, if accurate work is contemplated.

#### STOPPING POWER OF PHOTOGRAPHIC EMULSION

It seems appropriate to present a calculation of the stopping power of a photographic emulsion, based on the best data available on the atomic stopping power of the constituent atoms of the emulsion.

A method of calculating the stopping power for chemical compounds, when the stopping powers of the constituent atoms of the compound are known, has been outlined by several previous workers.<sup>23,24</sup> A brief review of the method of computing the stopping power of a chemical compound will be given before it is applied to the case of the photographic emulsion. The relative atomic stopping power of one substance, as compared with that of another substance taken as standard, may be defined by the relation

$$R_0/R = (N/N_0)(s/s_0), \quad (7)$$

where  $R_0$  is the range of a charged particle in air,

<sup>23</sup> H. R. Von Trautenberg, *Zeits. f. Physik* **5**, 396 (1921).

<sup>24</sup> P. Cüer, *Comptes rendus* **223**, 1121 (1946).

$R$  is the range in the test substance,  $N_0$  is the effective number of atoms per cubic centimeter of air under normal conditions and based on an average atomic weight, and  $N$  is the number of atoms per cubic centimeter of the test substance. The quantity,  $s/s_0$ , is the atomic stopping power of the substance relative to that of air. As pointed out by Cüer,<sup>24</sup> the quantity usually measured in experimental work is not  $R_0/R$  but the relative differential ranges,  $\Delta R_0/\Delta R$ , for small energy steps. Accordingly, we will change (7) to read

$$\Delta R_0/\Delta R = (N/N_0)(s/s_0), \tag{8}$$

or, since  $s_0$  for air is taken as unity,

$$\Delta R_0/\Delta R = (N/N_0)s. \tag{9}$$

If we replace the quantities  $N$  and  $N_0$  by their equivalent values expressed in terms of density and atomic weight, i.e.,  $N = kd/A$  and  $N_0 = kd_0/A_0$ , then the relationship

$$\Delta R_0/\Delta R = (dA_0/d_0A)s \tag{10}$$

follows. Bragg established the fact that the stopping power of a chemical compound made up of several types of atoms is an additive property. Accordingly, we can write for a compound

$$\Delta R_0/\Delta R = n(N_1s_1 + N_2s_2 + N_3s_3 \cdots + N_ks_k)/N_0$$

where  $N_1, N_2$ , etc., refer to the number of atoms of each type in one molecule, and  $n$  refers to the number of molecules of the compound per cubic centimeter. Since

$$N_0 = kd_0/A_0$$

and

$$n = d/(N_1A_1 + N_2A_2 + \cdots + N_ks_k),$$

we find

$$\frac{\Delta R_0}{\Delta R} = \frac{d \cdot A_0}{d_0} \left( \frac{N_1s_1 + N_2s_2 + \cdots + N_ks_k}{N_1A_1 + N_2A_2 + \cdots + N_ks_k} \right) = d \cdot A_0 S / d_0 M, \tag{11}$$

where  $M$  in Eq. (11) refers to the molecular weight and  $s$  to the molecular stopping power. For purposes of calculation, it is more convenient to write (11) in a slightly different form:

$$\Delta R_0/\Delta R = (d \cdot A_0/d_0) \{ (N_1A_1s_1/A_1 \sum_j N_jA_j) + \cdots + (N_ks_ks_k/A_k \sum_j N_jA_j) \}.$$

TABLE III. Composition of emulsion.\*

Element	Atoms per molecule of AgBr	Weight per mole of AgBr	$P_i$ weight percent	$P_i/A_i$	fractional weight atomic weight
Ag	1.0	107.88	47.20		0.004375
Br	1.0	79.92	34.95		0.004373
C	1.39	16.70	7.30		0.006083
H	3.06	3.08	1.35		0.013410
N	0.43	6.02	2.64		0.001886
O	0.932	14.90	6.53		0.004081

\* This emulsion contains no iodide but this fact affects the stopping power only slightly since bromide replaces the iodide. The effective composition of this emulsion, as it affects stopping power, is closely the same as the Eastman NTA and NTB plates and the Ilford plates.

This relationship may be abbreviated to read\*\*

$$\Delta R_0/\Delta R = (d \cdot A_0/d_0) \{ (p_1s_1/A_1) + (p_2s_2/A_2) + \cdots + (p_ks_k/A_k) \}, \tag{12}$$

where  $p_i = N_iA_i/\sum_j N_jA_j$  represents the fractional weight of each element contained in the compound.

The photographic emulsion is not a chemical compound in the sense that it is a homogeneous chemical combination of atoms composed of identical molecules. Rather, it is a highly dispersed mixture of two compounds, gelatin and silver bromide. The gelatin is a continuous medium in which the silver bromide is suspended in the form of tiny crystals. The physical characteristics of the emulsion, for which stopping-power calculations are here carried out, may be summed up in the following list of values:

Density of emulsion	3.64 g/cc
Percent weight of AgBr in dry emulsion	85.0 percent
Percent weight of gelatin	15.0 percent
Density of silver bromide	6.47 g/cc
Concentration of AgBr in emulsions	3.09 g/cc
Average diameter of grain	0.3 $\mu$
Mass of average grain	0.92 $\times 10^{-13}$ g
Number of grains/cc of emulsion	3.36 $\times 10^{13}$ grains/cc
Moisture content (percent weight of dry emulsion)	3.35 percent

If we assume that such a mixture of silver bromide grains and gelatin can be treated as a smoothed-over compound of the various constituent atoms, we can calculate the relative stopping power of an emulsion from Eq. (12), providing we know the atomic composition of the

\*\* This formula was also used by P. Cüer (see reference 24) for calculating the stopping power of emulsions.

TABLE IV. Atomic stopping-power values.

Energy Mev		Atomic stopping power						
$E_\alpha$	$E_H$	$S_{Ag}$	$S_{Br}$	$S_C$	$S_H$	$S_N$	$S_O$	$S_{air}$
2.07	0.52	2.25	2.07	0.94	0.260	1.02	1.10	1.0
4.66	1.17	3.08	2.68	0.932	0.224	1.02	1.10	1.0
8.30	2.09	3.43	2.94	0.921	0.209	1.01	1.10	1.0
12.95	3.26	3.64	3.10	0.914	0.200	1.01	1.09	1.0
18.60	4.70	3.76	3.19	0.908	0.194	1.00	1.09	1.0
33.20	8.36	3.93	3.30	0.899	0.186	1.00	1.08	1.0
51.90	13.06	4.04	3.38	0.892	0.181	.99	1.08	1.0
Extrapolated								
80.0	20.0	4.12	3.44	0.850	0.170	0.98	1.07	1.0

emulsion and the atomic stopping powers of the atoms involved. To illustrate this, the following calculation of stopping power *versus* energy has been made.\*\*\*

The atomic composition of an emulsion which is made up of 85 percent silver bromide, has a moisture content of 3.35 percent of the dry weight of the emulsion, and contains gelatin composed of 50 percent carbon, 6.7 percent hydrogen, 18 percent nitrogen, and 25 percent oxygen is given in Table III. A table of atomic stopping powers of the elements hydrogen, carbon, aluminum, copper, silver, and gold as a function of energy for alpha-particles and protons has been published by Bethe and Livingston.<sup>25</sup> By drawing curves relating stopping power and atomic weight from these published values, interpolated values of atomic stopping

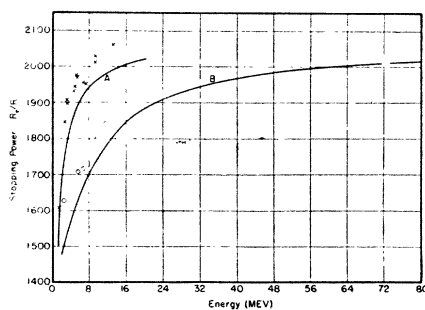


FIG. 9. Calculated integral stopping-power *versus* energy curves for nuclear-track emulsion: (a) for protons, (b) for  $\alpha$ -particles. Experimental points from paper by Lattes, Fowler, and Cür, Proc. Roy. Soc. 59, 883 (1947).

\*\*\* The following procedure for calculating the stopping power of a heterogeneous emulsion follows closely a method worked out (unpublished) by my colleague, Dr. Amos Newton, to whom the author wishes to express his indebtedness.

<sup>25</sup> H. Bethe, and M. S. Livingston, Rev. Mod. Phys. 9, 272 (1937).

power for bromine, nitrogen, and oxygen can be obtained. The published values, along with the values obtained therefrom by interpolation, are set down in Table IV.

The stopping power of the emulsion relative to air was calculated for each energy value in Table IV, using Eq. (12), and values of the constants: average atomic weight of air ( $A_0$ ) = 14.5; density of air ( $d_0$ ) = 0.001205 g per cubic centimeter; density of emulsion ( $d$ ) = 3.64 g per cubic centimeter; and the atomic stopping-power values,  $s_i$ , given in Table IV.

The values of the relative stopping power,  $\Delta R_0/\Delta R$ , so obtained for alpha-particles and protons of various energies are given in Table V.

In Fig. 9 the integral stopping power,  $R_0/R$ , for both protons and alpha-particles is plotted as a function of energy in Mev. The values for plotting these curves were obtained as follows: Differential-range values in air over narrow energy steps (2 Mev) were divided by the stopping-power values in Table V to obtain the corresponding range values in the emulsion. These values were then summed over discrete energy steps to obtain integral-range values in the emulsion. The quotients of the integral-range values in air and in the emulsion give the integral stopping-power values. The experimental points shown in Fig. 9 are values of stopping power that were published by Lattes, Fowler, and Cür<sup>26</sup> for the Ilford B-1 emulsion. The silver halide content of this emulsion, according to the Ilford data given earlier in this paper, is 81 percent. The concentration of silver bromide in the emulsion used in the present calculations (with 3.35 percent water) is, according to Table III, 82.05 percent. Thus, since the silver halide concentration is closely the same in the two cases, the experimental points serve to show the order of accuracy\*\*\*\* to be expected

<sup>26</sup> C. M. G. Lattes, P. H. Fowler, and P. Cür, Proc. Phys. Soc. (London) 59, 883 (1947).

\*\*\*\* The theoretical stopping-power curve of Fig. 9 for alpha-particles also agrees fairly well with the data of Tsien San-Tsiang, Chastel, Faraggi, and Vignoron (see reference 19) on Ilford halftone concentrated plates given earlier in this paper. Peck (see reference 38) made measurements of stopping power on the Eastman NTB emulsion for protons of energy 2-9 Mev. From 9 Mev to 4 Mev he found a constant value of stopping power of about 2050. However, his measurements showed a sharp rise of stopping power below 4 Mev, going up to 2820 at 2.4 Mev. These results are not understood at present, but since they are in sharp variance with both theory and experimental

from theoretically calculated stopping-power values.

In Figs. 10 and 11, the curves of Fig. 9 have been converted to give stopping power,  $R_0/R$ , versus range in microns in the emulsion. In Fig. 12, theoretical range-energy curves for protons and alpha-particles in the photographic emulsion are given based on the variable stopping-power values,  $R_0/R$ , from the curves of Fig. 9.

It is of interest at this point to give the results of calculations of stopping power,  $\Delta R_0/\Delta R$ , as a function of energy for pure silver bromide. Using Eq. (12) and values of the atomic stopping power for silver and bromine from Table IV, the values of stopping power shown in Table VI were obtained. It is to be noted that the stopping power for silver bromide is considerably higher (~50 percent) than that for the emulsion itself.

**DENSITY OF PHOTOGRAPHIC GRAINS IN TRACKS OF NUCLEAR PARTICLES**

The question of the density of developed grains in a nuclear track recorded by the photographic emulsion is of great importance to the nuclear physicist employing the photographic technique for registration of charged particles. By the grain spacing, the type of particle under investigation can frequently be recognized directly. For example, the grain spacing and small angle scatter make it possible to distinguish unmistakably the tracks of a meson and a proton.<sup>13, 16</sup> The grain spacing may be assumed to depend upon the energy-loss curves shown in

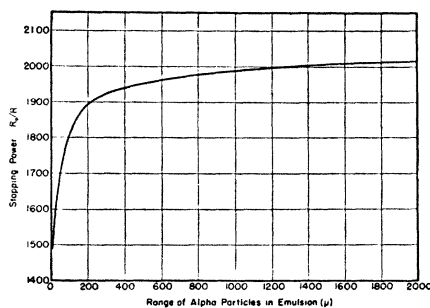


FIG. 10. Calculated integral stopping-power versus range curve of nuclear-track emulsion for protons.

results of other workers, it would appear that there must have been some unusual circumstances in the experimental work or the particular emulsion used that gave this behavior. Only by further careful measurements along these lines can this problem be cleared up.

TABLE V. Stopping power of emulsion.

Energy Mev		$\Delta R_0/\Delta R$
$E_\alpha$	$E_H$	
2.07	0.52	1511
4.66	1.17	1764
8.30	2.09	1868
12.95	3.26	1930
18.60	4.70	1964
33.20	8.36	2009
51.90	13.06	2040
Extrapolated		
80	20	2065

Fig. 3. At points on these curves of the same energy loss, it is to be expected that the grain spacing will be substantially the same, regardless of the type of particle. This is true because the action of the incident particles in producing a latent image in the photographic grain is dependent upon the number of ions produced in the individual grain. In this respect, the process of latent-image formation with particle radiation is not materially different from that in the case of light.

It is now well established<sup>27-29</sup> in the cases of light exposure that the individual grains of the emulsion act as units in exposure. The light quanta strike a silver bromide crystal in succession, and each quantum, upon absorption, raises the energy state of an electron attached to a bromine ion into an empty state of the conduction band of silver bromide. An electron with energy corresponding to a level of the conduction band can move about freely in the crystal and

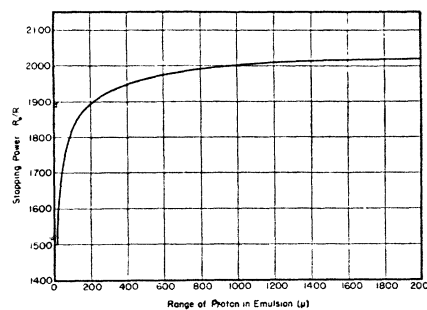


FIG. 11. Calculated integral stopping-power versus range curve of nuclear-track emulsion for alpha-particles.

<sup>27</sup> R. W. Gurney, and N. F. Mott, Proc. Roy. Soc. (London) **164A**, 151 (1938).

<sup>28</sup> J. H. Webb, J. App. Phys. **11**, 18 (1940).

<sup>29</sup> W. F. Berg, and K. Mendelssohn, Proc. Roy. Soc. (London) **168A**, 168 (1938).

TABLE VI. Stopping power of silver bromide.

Energy Mev		$\Delta R_0/\Delta R$
$E_\alpha$	$E_H$	
2.07	0.52	1796
4.66	1.17	2394
8.30	2.09	2648
12.95	3.26	2802
18.60	4.70	2890
33.20	8.36	3006
51.90	13.06	3085
80	20	3164

can be shifted under the action of an electric field. This has been amply demonstrated by experiments on the photo-conductance properties of the silver bromide crystal. Such an electron will move about in the crystal until it comes into contact with a so-called sensitivity speck (a small clump of impurity atoms or a distorted place in the crystal) in the grain, where it becomes trapped in a lower energy level, below the conduction band. An electron trapped in this way is surrounded by an electrostatic field which will attract any positive silver ions in the neighborhood. Since there are always some mobile silver ions present in the silver bromide crystal, as shown by studies on the ionic conductivity of these crystals at room temperature, these ions move up to the charged speck, where they join with the electron to form a silver atom. This process is repeated until a speck of silver is formed large enough to initiate development. It seems likely that exposed grains may acquire a number of silver specks of varying sizes; however, the grain becomes developable only when it has acquired at least one silver speck large

enough, and properly located, to initiate development of that grain.

In the case of exposure of grains to high-velocity, charged particles, the production of electrons in the grain takes place upon passage of the particle through the grain. Electrons freed by such means will behave, in general, like those produced by exposure to light and may be expected to form a latent image. One point of difference should be emphasized, however. With high-energy particles, the electrons are formed within the grain in a very short time, e.g., with a 5-Mev alpha-particle and a grain size of  $0.3\mu$  diameter, all the electrons are freed in about  $2 \times 10^{-14}$  second. This rapidity of liberation of the electrons may lead to inefficiency in the photographic process. First, because the positive and negative ions formed by the particle lie along a straight, narrow path through the grain, there will be a tendency for the ions to recombine and thus to be lost for the latent-image formation. Second, it is well known that light exposures become less efficient at very short exposure times (below  $10^{-3}$  second), because of the failure of the reciprocity law in the photo-chemical process of latent-image formation. For the latent-image formation to proceed efficiently, electrons should be freed at such a rate that the ionic movement of the silver ions can keep pace with the electronic process and thus neutralize the electrons as fast as they become trapped. If the exposure is given too fast, the latent-image silver has a tendency to be dispersed throughout the grain, which introduces competition between specks and inefficiency in the process.

The foregoing brief description of the theory of latent-image formation will serve as a basis for considering why the grain spacing in photographic tracks is different with particles of different charge but with the same velocity, and with identical particles having different velocities.

In Fig. 13 is shown schematically an electron revolving about an atom of the stopping material and a charged particle of charge,  $ze$ , and velocity,  $v$ , passing this electron at a distance,  $p$ . The force experienced by the electron while the charged particle is in the vicinity will be of the order of magnitude,

$$F = (ze)^2/p^2.$$

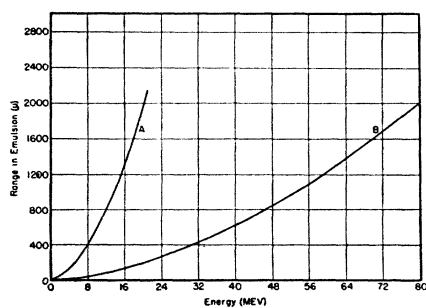


FIG. 12. Calculated range-energy curves for (A) protons and (B)  $\alpha$ -particles in nuclear-track plate. Drawn for variable stopping-power values from calculated curves in Fig. 9.

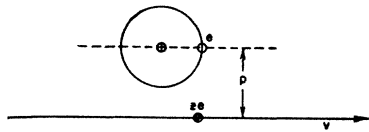


FIG. 13. Schematic diagram to illustrate impulse given to an electron by passage of a charged particle.

The impulse experienced by the electron is given by the product of the force,  $F$ , and the time,  $t$ , that the particle spends in the neighborhood of the electron. To a first approximation, this time may be taken as

$$t = 2p/v.$$

Thus, the impulse is

$$Ft = ze^2/pv. \tag{13}$$

Let us now consider the impulse given to an electron in the two cases: (1) by the passage of a proton, and (2) by an alpha-particle, both of the same range. It is known that an alpha-particle and a proton of the same range have the same velocities. This follows because the alpha-particle, though it has four times the energy of the proton, loses energy at four times the rate of the proton because of its double charge, as can be readily seen by reference to Eq. (1). If, now, we equate impulses in these two cases, we find that

$$2e^2/p_{\alpha}v = e^2/p_Hv,$$

from which

$$(p_{\alpha}/p_H)^2 = 4.$$

It is readily seen that  $p_{\alpha}$  and  $p_H$  define cylinders of equivalent action of the alpha-particle and proton, respectively. The number of atoms contained in such cylinders will be proportional to the  $p^2$  values. Thus, it may be expected that, for equal velocities, the alpha-particle will ionize approximately four times as many atoms as the proton.

Similarly, it is well known that the velocities of protons and deuterons of the same range have velocities in the ratio,  $v_H = 1.25v_d$ . The ratio of the  $p$  values in this case, since the charges are equal, will be 1.25. Consequently, the deuterons will produce  $(1.25)^2$ , or 1.56 times as many ions as a proton of the same range.

The threshold sensitivity of a photographic grain must depend in first approximation upon the number of ion pairs produced in the grain.

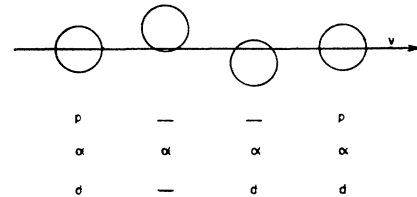


FIG. 14. Schematic diagram to illustrate passage of a charged particle through irregularly distributed photographic grains.

With this basic assumption, the schematic diagram in Fig. 14 can be used to explain crudely the action of different particles on grain spacing. Assume, for example, that a nuclear particle of a given range follows the path shown by the arrow. This path is seen to pass through different thicknesses in different grains, which are irregularly distributed in space. Suppose the particle is a proton and of such velocity that it can produce sufficient ions in the grain to form a latent image only if it passes through a full diameter of the grain. Then, since the path shown passes through the full thickness of the two end grains, a proton following the path would make grains 1 and 4 developable. A deuteron of the same range, having lower velocity, and thus somewhat higher ionizing power, will perhaps affect grains 1, 3, and 4. An alpha-particle of the same range, however, having the same velocity and thus four times the ionizing power of the proton, will affect all grains in the path, 1 to 4.

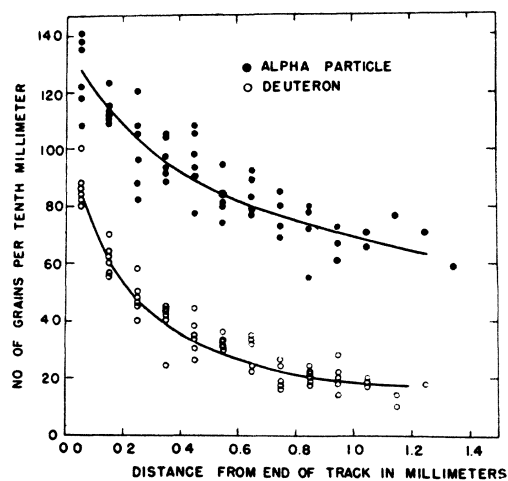


FIG. 15. Curves showing grain spacing as a function of distance from end of particle track. From paper by Brock and Gardner (see reference 32).

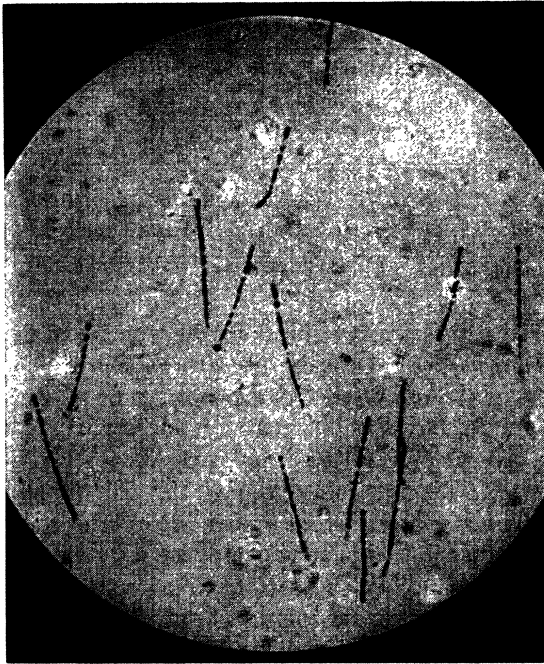


FIG. 16. Tracks of Po  $\alpha$ -particles obtained with Eastman NTA plate.

Grain spacings in alpha-particle, deuteron, and proton tracks were measured by Wilkins and St. Helens<sup>30</sup> for equal residual ranges, and it was found that the grain density in the proton tracks was about one-half that for the alpha-particle and that the grain density of the deuteron tracks fell between that of the proton and alpha-particle tracks.

When charged particles, such as alpha-particles (<10 Mev) and protons (<3 Mev), have very low velocity, they are highly ionizing and will affect practically every grain with which they come in contact. Under these conditions, the density of grains in a track will approach a maximum value set by the grain population of the unexposed emulsion. Perhaps it will be of interest in this connection to give the maximum grain density in terms of the silver bromide concentration,  $C$ , and the diameter of the grain,  $d$ , for an emulsion of the conventional type. If it is assumed that all grains are spherical and of diameter,  $d$ (cm), then a little reflection will show that the number of grains that will be hit

by a particle traveling in a straight path of length,  $\lambda$ (cm), will be equal to the total number of grains whose centers are contained within a cylinder of diameter,  $d$ , and length,  $\lambda$ . This number is readily found by dividing the silver bromide concentration of the emulsion,  $C$  grams per cubic centimeter, by the mass of one grain and multiplying by the volume of the cylinder of diameter,  $d$ , and length,  $\lambda$ . The resulting expression is

$$n = \frac{3}{2}(C\lambda/d\rho) \text{ grains per centimeter,} \quad (14)$$

in which  $\rho$  represents the density of silver bromide in grams per cubic centimeter. If we take  $\lambda$  to be 1 cm and  $\rho$  to be 6.47, we obtain, for the maximum grain density,

$$n = 0.23(C/d) \text{ grains per centimeter.} \quad (15)$$

This relation was first given and tested by Idanoff<sup>31</sup> and subsequently tested by Demers.<sup>4</sup> Idanoff, using several emulsions with different values of  $C$  and  $d$ , tested the relation (15) by measuring the relative grain spacings,  $\Delta$ . If we set

$$\Delta = 1/n = d/0.23C, \quad (16)$$

then

$$\Delta_1/\Delta_2 = (d_1/d_2)(C_2/C_1),$$

and the relation between  $\Delta$  values for different emulsions has been found to hold fairly accurately. Also, Demers<sup>4</sup> tested the relation (16) for a number of commercial emulsions and for special experimental emulsions made by his own formulas and found that the minimum grain-spacing,  $\Delta_0$ , for alpha-particles near the end of their range was in fair agreement with the theoretical minimum grain spacing,  $\Delta$ , calculated from (16).

It is of interest to calculate the value of  $\Delta_0$  for the emulsion for which the stopping-power calculations were made earlier in this paper. Using the values  $C = 3.09$  g per cubic centimeter and  $d = 0.3\mu$ , we find that

$$\Delta_0 = d/0.23C = 0.435\mu.$$

In Fig. 15 are shown experimental data on grain density as a function of residual path length for Eastman NTA plates obtained by

<sup>30</sup> T. R. Wilkins, and H. J. St. Helens, *Rev. Mod. Phys.* **11**, 35 (1940); *Phys. Rev.* **54**, 783 (1938).

<sup>31</sup> A. Idanoff, *J. de phys. et rad.* **6**, 283 (1935); *Comptes rendus (Doklady) U.R.S.S.* **28**, 110 (1940).



Brock and Gardner<sup>32</sup> of the Radiation Laboratory of the University of California. The points represent numbers of grains per 0.1-mm path length for varying residual path for both alpha-particles and deuterons. It may be seen that the grain density for the deuterons is less than that for the alpha-particles throughout the range covered. In the case of the alpha-particles, at the shortest residual ranges measured the grain density is about 1.5 grains per micron, corresponding to a  $\Delta$  value of  $0.6\mu$ .

A useful concept has been employed by Lattes, Occhialini, and Powell<sup>6</sup> for determining from grain density the relative masses of two types of particles of the same charge value. It is a well-known fact (see Eq. 5) that the rate of energy loss of a charged particle having fixed charge value is a function of the velocity of the particle only, irrespective of the mass of the particle. Thus, the rate of energy loss may be written

$$dE/dR=f(v). \quad (17)$$

Since the photographic effect is dependent upon the rate of energy loss, it can be assumed that the grain density along the track will also be a function of velocity, thus

$$dN/dR=f(v).$$

From Eq. (5), it can be seen that the residual track length,  $R$ , of a particle of given velocity,  $v$ , and fixed charge, is proportional to its mass,  $M$ . Thus, the grain density may also be written as a function of residual range divided by  $M$ ,

$$dN/dR=f(R/M). \quad (18)$$

Integrating, we find that

$$N=M\int_0^{R/M} f(R/M)d(R/M). \quad (19)$$

Since the integral on the right would have a unique value, starting from a point on the track where the velocity has a given value (given  $R/M$  value), then, for two different particles having different masses the total numbers of grains,  $N_1$  and  $N_2$ , in the residual paths,  $R_1$  and  $R_2$ , will be in the ratio of the masses,  $M_1$  and  $M_2$ . Thus,

$$R_1/R_2=N_1/N_2=M_1/M_2. \quad (20)$$

<sup>32</sup> R. L. Brock and E. Gardner, Rev. Sci. Inst. 19, 299 (1948).

If it is desired to compare masses of two particles from grain counts, the procedure is to find points along the two trajectories for which the grain densities are equal. Then the relative masses of the two particles will be in the ratio of the two residual paths, or, alternatively, in the ratio of the total numbers of grains in the two residual paths.

#### ANALYSIS OF NUCLEAR TRACKS AND PLATE CALIBRATION

In analyzing the tracks of nuclear particles recorded in the photographic emulsion, the experimenter must rely upon such features as the recorded range of the particle in the emulsion, small angle scattering along the track, and the grain spacing along the track. The actual range of the particle and the small angle scattering will depend upon the composition of the emulsion and hence may be expected to be constant from one emulsion to another. However, the recorded range of a particle and the grain spacing at the beginning of the track will depend upon the

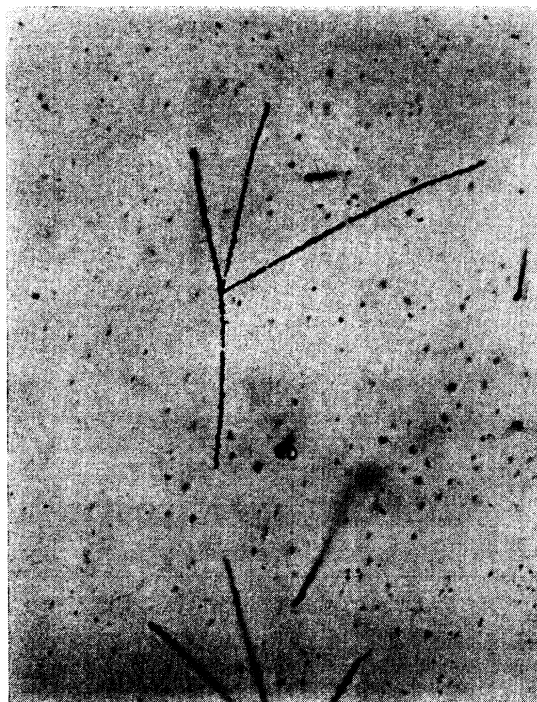


FIG. 17. Tracks of four  $\alpha$ -particles from thorium atom disintegrating through the series: ThX (5.68 Mev), Tn (6.28 Mev), ThA (6.78 Mev) and ThC' (8.78 Mev).

sensitivity of the individual grains of the emulsion, which is very difficult to reproduce accurately. Accordingly, if the photographic plate is to be used as a quantitative tool to evaluate

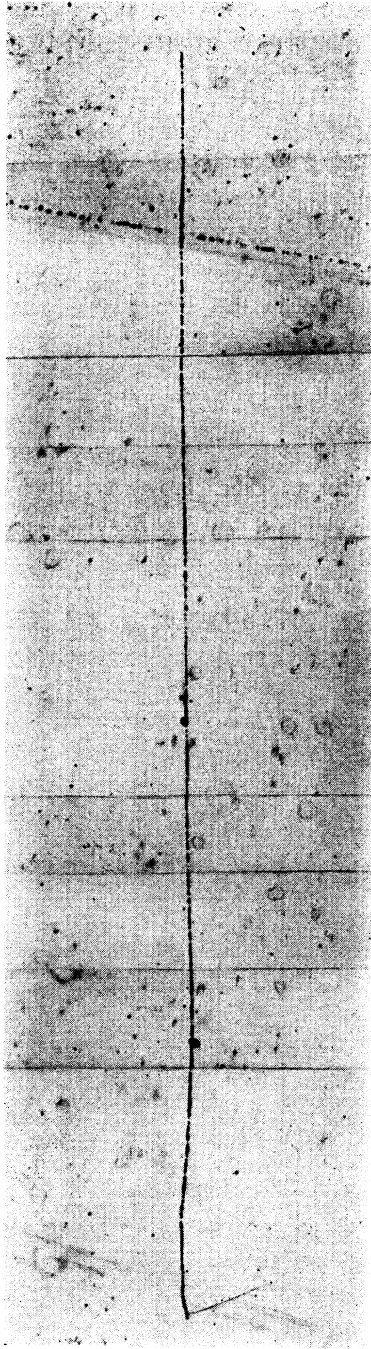


FIG. 18. Track of a 7-Mev proton in Eastman NTB emulsion. Track ends at bottom of figure.

the properties of a particle through range and grain-spacing measurements, it is essential that the plates used in such experiments be given control exposures to particles of known characteristics, for example, protons or alpha-particles of a series of known energy values, and processed in a controlled manner. All plates coated from a single emulsion batch can be relied upon to give closely uniform results, provided they have been stored under proper temperature and humidity conditions prior to exposure and provided they receive proper and uniform handling during exposure and processing.

It is highly desirable that emulsions supplied by the manufacturer be constant from batch to batch, so that a minimum of calibration exposures will be required. In the preparation of the nuclear-track plates, serious efforts are being made to achieve this end. However, up to the present time, much experimental work has been necessary to improve these plates in various ways, such as to increase their sensitivity to higher energy particles, to lower the background density, and to reduce the latent-image fading that takes place between exposure and development. During this period of experimentation, the Eastman NTB plate, for example, has been designated as an "experimental plate."

As was stated earlier in this paper, successive batches of Eastman NTA plates are given a standardized test to polonium alpha-particles (5.3 Mev) and the Eastman NTB plates are given a standardized test to 7-Mev protons. These tests are used as a control measure to screen out those emulsions which fall outside certain tolerances in recorded range-value and grain-spacing quality of the tracks. However, it must be pointed out that such tests are inadequate to determine the uniformity of behavior of emulsions when exposed to particles of energy greatly exceeding those used in the tests. For example, it has been found that nuclear-track plates that have shown very uniform grain spacing from one emulsion to another when tested to moderate energy protons may show non-uniform results when exposed to particles of higher energy approaching the threshold sensitivity value of the plate. At higher energies where the grain density in the tracks becomes sparse, the grain spacing becomes much more

critically dependent upon the threshold sensitivity of individual grains and even small differences in sensitivity begin to show up in a measurable way. In the near future, the new cyclotron of the University of Rochester will be in operation, and it is hoped that it will then be possible to give standardized tests to protons over much wider energy ranges than has been possible in the past.

At present, the only safe procedure that can be recommended to the worker in this field is to calibrate the plates of each new emulsion batch in the energy range that the plates are to be used. Accordingly, it is suggested that, if an extended investigation is to be carried out, plates in sufficient quantity to complete the work be acquired in the beginning from one emulsion number and stored at reduced temperature until used.

**EXAMPLES OF NUCLEAR TRACKS IN THE PHOTOGRAPHIC EMULSION**

As examples of tracks obtained on commercial nuclear-track plates, the pictures in Figs. 16-19 are shown.

The tracks in Fig. 16 were obtained on an Eastman NTA emulsion by means of a weak polonium source of alpha-particles placed practically in contact with the photographic emulsion. The polonium alpha-particles have an energy of 5.3 Mev and, accordingly, a range of about  $22\mu$  in the emulsion.

The star tracks in Fig. 17 represent four alpha-particle tracks from a disintegrating thorium atom. An Eastman NTA plate was impregnated with a solution of thorium nitrate, dried, left for a few days, and then washed and processed. A plate so treated will show stars produced by alpha-particles from a single center, corresponding to successive disintegrations of the thorium nucleus. The four tracks shown in this figure correspond to the four successive alpha-disintegrations of thorium X (5.68 Mev), thoron (6.28 Mev), thorium A (6.78 Mev), and thorium C' (8.78 Mev).

Figure 18 shows the track of a 7-Mev proton on an Eastman NTB plate. The grain spacing throughout this track is about constant, indicating that the full grain density was obtained over its entire length. The direction of the proton travel is downward, as shown by the

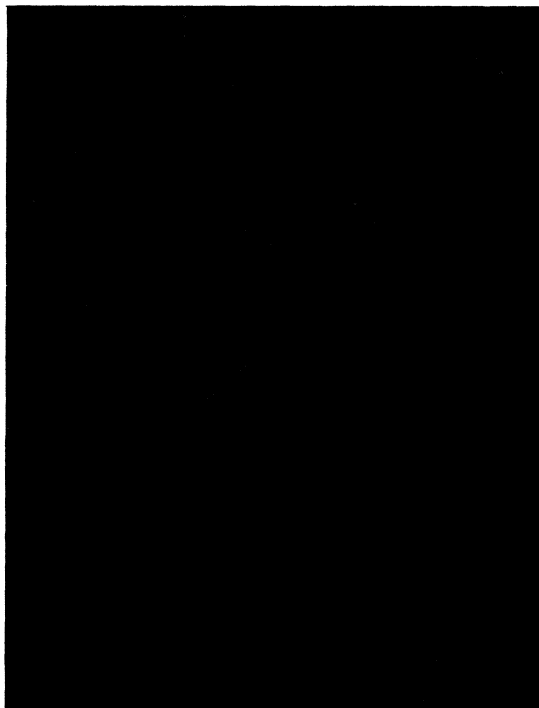


FIG. 19. Track of  $U^{235}$  fission on Eastman NTC emulsion, obtained by impregnating emulsion with uranium acetate and bombarding with slow neutrons.

small angle scattering at the lower end which occurs when its velocity is low.

Figure 19 shows the paths of the two fission fragments from a  $U^{235}$  atom. An Eastman NTC plate was impregnated with uranium acetate and bombarded with low speed neutrons. The fission of the  $U^{235}$  atom occurred near the center of the track and the track itself was produced by the two highly charged fragments flying apart, with a combined energy of 160 Mev. The high charge on these fragments is manifested by the rela-

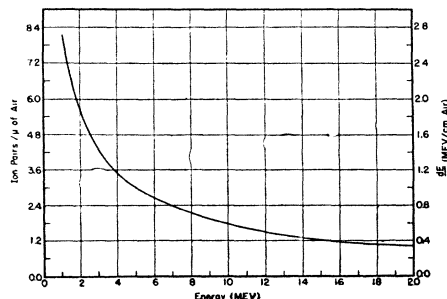


FIG. 20. Ion-pair production *versus* energy curve for  $\alpha$ -particles in air.



FIG. 21. Tracks of electrons in Eastman NTB emulsion. Plate exposed to 180 kv x-rays to produce photoelectrons.

tively short path of these tracks ( $25\mu$  for the combined fragments). Also, it is to be noted in this case that the grain density is highest near the center of the track and falls off toward the two extremities as the charge on the fragments, and thus the ionizing power, is reduced.

#### ION-PAIR PRODUCTION AND LATENT-IMAGE FORMATION

In concluding this paper it seems appropriate to make a few remarks about the mechanism of latent-image formation under the action of charged particles.<sup>33</sup> By analogy with the action of light on the photographic grain, it appears almost certain that the action of charged particles in producing a latent image in the photographic grain results from the production of free conduction electrons just as in an exposure to light. There are certain differences, however, which should be mentioned. In an exposure to

light, the quanta are absorbed at random points over the entire grain surface and usually at a moderate rate such that all the quanta received by one grain are absorbed in a time greater than  $10^{-3}$  second. However, as we pointed out earlier in the case of a charged particle of even moderate energy, all ion pairs are produced along a straight line through the grain and in a time less than  $10^{-13}$  second. Under these conditions, formation of the latent image is attended by inefficiency because of ion recombination and reciprocity-law failure. For both these reasons it is to be expected that more electrons must be released in a grain to render it developable with an exposure to a charged particle than is the case in an exposure to light.

In Fig. 20 a curve is shown giving the number of ion pairs formed per micron of path length in air for an alpha-particle of varying energy. This curve was obtained by plotting the differential values of ion-pair production from published tables.<sup>34</sup> This curve is known to follow the same course as the energy-loss curves shown in Fig. 3. Accordingly, a scale has been given on the right-hand ordinate axis of Fig. 20 specifying the energy loss in Mev per centimeter. In air, about 35 ev is required to produce each ion pair, and this figure has been found to be very closely the same, whether the incident particle is an electron, a proton, or an alpha-particle.

The production of ion pairs on passage of a charged particle through solid materials will also take place in accordance with a curve like that of Fig. 20. However, this quantity is not nearly so easily measured in a solid as in a gas, and there are very few data available on the energy required to produce an ion pair in solid materials. Experiments with the recently developed crystal counters, using silver chloride crystals as a solid ionization chamber for the detection of high-energy charged particles, offer the possibility of obtaining the average value of energy required to produce an ion pair in silver chloride. Since silver chloride is very similar to silver bromide, the value obtained in this way will also apply in the photographic case. VanHeerden,<sup>35</sup> who de-

<sup>33</sup> For additional information see the detailed discussions of the problem of latent-image formation by charged particles which have been prepared by P. Cüer, *Sci. et Ind. Phot.* **18**, 321 (1947); **18**, 353 (1947).

<sup>34</sup> J. B. Hoag, *Electron and Nuclear Physics* (D. Van Nostrand Company, Inc., New York, 1938), second edition, p. 464.

<sup>35</sup> P. J. VanHeerden, *N. V. Noord-Hollandsche Uitgevers Maatschappij* (Amsterdam, 1945).

veloped the silver chloride crystal counter, found that 7.6 ev is required to produce each ion pair for the case of high-speed beta-particles passing through the silver chloride crystal. More recently, Hofstadter, Milton, and Ridgeway,<sup>36</sup> working with the silver chloride crystal counter and using high-energy electrons, found a series of values for the energy per ion pair with different crystal samples. The lowest value obtained was 13–16 ev, and the authors considered this value to be higher than the true value because of imperfections in the crystal which are known to limit the photo-conductance current. It appears that VanHeerden's value of 7.6 ev is the best available at present for the energy required to produce an ion pair in silver chloride and this value will be used here for the purpose of calculation.

We note from the curve of Fig. 20 that for an 18-Mev alpha-particle, ion-pair production in air amounts to 1 ion pair per micron of air and the energy loss amounts to approximately 0.35 Mev per centimeter of air. If we take the threshold sensitivity value of the photographic grain to be 0.013 Mev per centimeter of air, corresponding to a 100-Mev deuteron, this will give an ion-pair formation rate of 0.037 ion pair per micron of air, since ion-pair production is proportional to energy loss. The maximum number of ion pairs produced in a photographic grain for a particle of this same energy-loss value can be found by multiplying the number of ion pairs per micron of air by the stopping power of silver bromide relative to air ( $\sim 3000$ ), dividing by the ratio of electron volt per ion pair in silver bromide to electron volt per ion pair in air, and multiplying by the diameter of the grain ( $0.3\mu$ ). Then we find that

$$\begin{aligned} \text{Ion pairs/grain AgBr} &= 0.037 \times 3000 \\ &\quad \times (35/7.6) \times 0.3 = 153, \end{aligned}$$

as an approximate value of the threshold number of ions to produce developability of a photographic grain  $0.3\mu$  in diameter. This figure must be considered as only approximate, since an accurate threshold cannot be set for the highest energy particle that will produce developability of a grain. All that is known, e.g., is that the

<sup>36</sup> R. Hofstadter, J. C. D. Milton, and S. L. Ridgeway, *Phys. Rev.* **72**, 977 (1947).



FIG. 22. Track of a negative meson (mass = 300 me) in Eastman NTB emulsion. Range in emulsion 400 microns. Exposure made on University of California cyclotron.

beginnings of tracks of 100-Mev deuterons consist of widely and irregularly spaced grains, thus making it appear that we are reaching the limit at which a useful fraction of grains is being made developable.

It is interesting to compare the figure, 153 ions per grain, with the number of quanta absorbed per grain for developability, as determined from recent work on single-grain-layer plates.<sup>37,38</sup> In this work experimental data indicated that, on the average, 40 quanta had to be absorbed by a grain to produce developability.

Between the time of preparation of this paper and its printing, the sensitivity of nuclear-particle plates has been substantially increased. The highest sensitivity emulsions will now record electron tracks<sup>38</sup> up to 20–30 $\mu$ , corresponding to 50- to 70-kev energy.

In Fig. 21 are shown electron tracks obtained on an Eastman NTB plate exposed to 180-kv x-rays. The paths of photoelectrons ejected by the x-rays are recorded. The longest tracks registered here have a length of 20 $\mu$ , corresponding to approximately 50-kev energy. This plate was developed in D-8 developer diluted 2:1 for two minutes. The electron tracks afford such a convenient and sensitive method of testing the threshold sensitivity value of plates that this method is now being used for testing the Eastman NTB plate.

In Fig. 22 is shown the track of a meson recorded on an Eastman NTB plate. The ex-

posure was made to the mesons generated in the University of California cyclotron. The track shown is 400 $\mu$  in length and corresponds to a negative meson of mass 313 me and energy of approximately 3.6 Mev. It may be observed that the meson track ends in a star formation due to a nuclear reaction set off by the meson.

#### ACKNOWLEDGMENT

The author desires to express his appreciation to his colleague, Dr. J. Spence, for furnishing various experimental data on the nuclear-track plates, for the preparation of the microscopic pictures of all the particle tracks herein presented, and for valuable discussions throughout the course of the writing of this paper. It is a pleasure to express, on behalf of the Kodak Research Laboratories, appreciation to the Physics Department of the University of Rochester and to the Radiation Laboratory of the University of California for their kind cooperation in exposing Eastman Nuclear Track Plates to charged particles from their high-energy accelerators. In this connection, Mr. Norton, of the University of Rochester, and Dr. E. Gardner, of the University of California, deserve special thanks for their generous and cordial cooperation. The author also desires to express his thanks to Dr. E. Gardner, of the University of California, Dr. Amos Newton, of the Eastman Kodak Company, for helpful suggestions, and to Dr. M. Blau, of Columbia University, for advice on processing of nuclear-track plates.

<sup>37</sup> J. H. Webb, *J. Opt. Soc. Am.* **38**, 312 (1948).

<sup>38</sup> R. A. Peck, Jr., *Phys. Rev.* **72**, 1121 (1947).

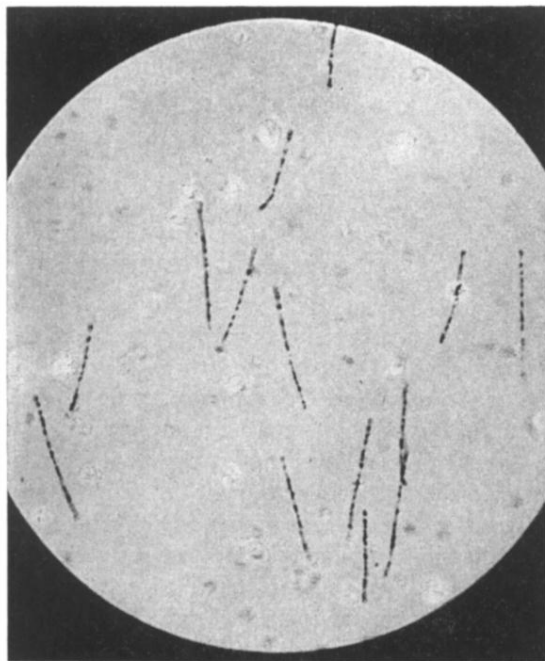


FIG. 16. Tracks of Po  $\alpha$ -particles obtained with Eastman NTA plate.

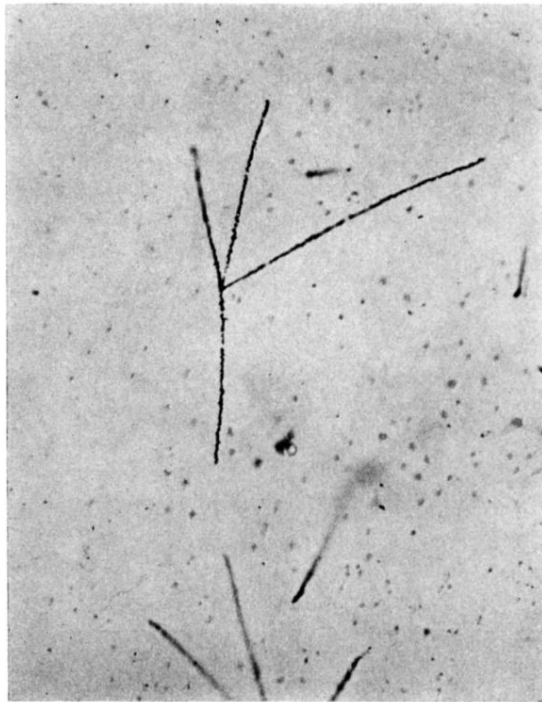


FIG. 17. Tracks of four  $\alpha$ -particles from thorium atom disintegrating through the series: ThX (5.68 Mev), Tn (6.28 Mev), ThA (6.78 Mev) and ThC' (8.78 Mev).



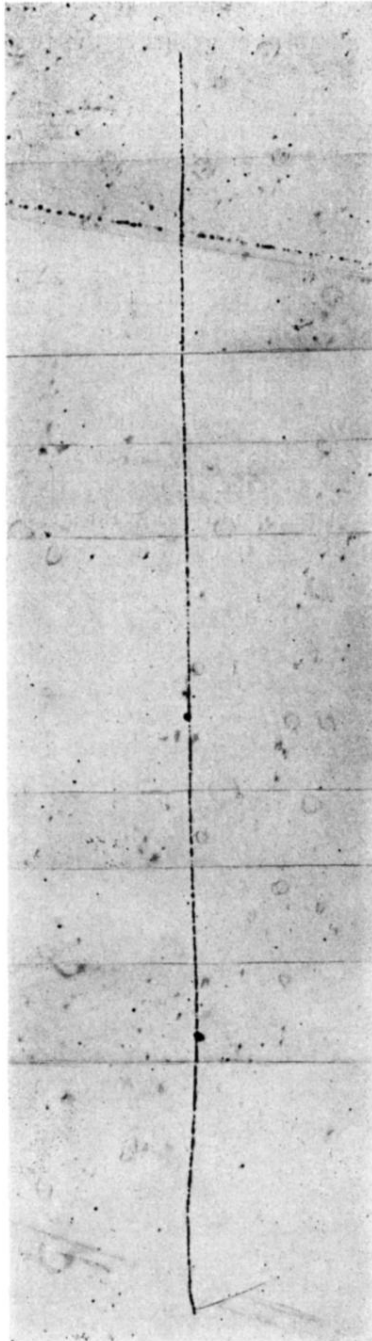


FIG. 18. Track of a 7-Mev proton in Eastman NTB emulsion. Track ends at bottom of figure.



FIG. 19. Track of  $U^{235}$  fission on Eastman NTC emulsion, obtained by impregnating emulsion with uranium acetate and bombarding with slow neutrons.

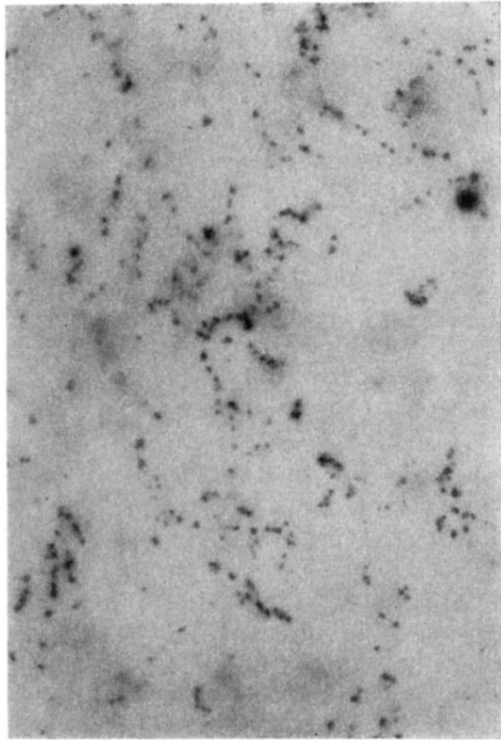
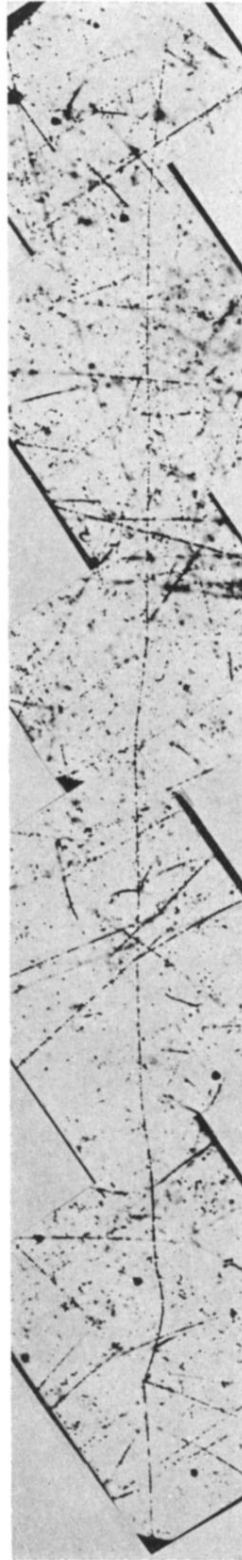


FIG. 21. Tracks of electrons in Eastman NTB emulsion. Plate exposed to 180 kv x-rays to produce photoelectrons.

FIG. 22. Track of a negative meson (mass = 300 me) in Eastman NTB emulsion. Range in emulsion 400 microns. Exposure made on University of California cyclotron.



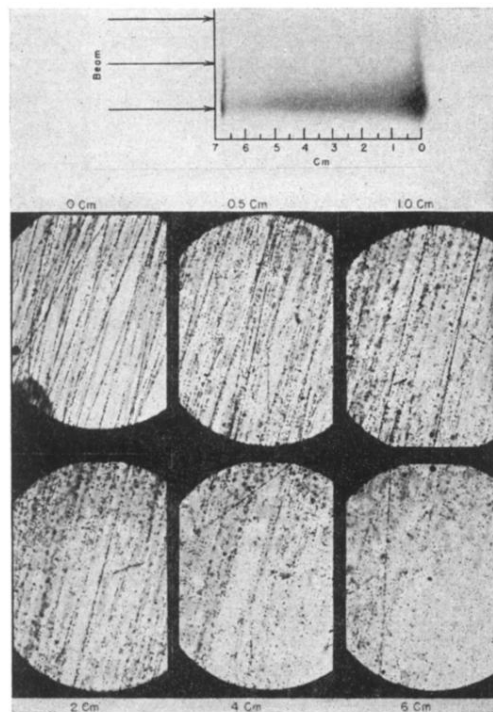


FIG. 4. Photographic effect of 190-Mev deuterons on nuclear-track plates. Upper picture=over-all density due to deuterons as they are slowed. Lower picture=photomicrographs of tracks of deuterons at various distances from the stopping end.

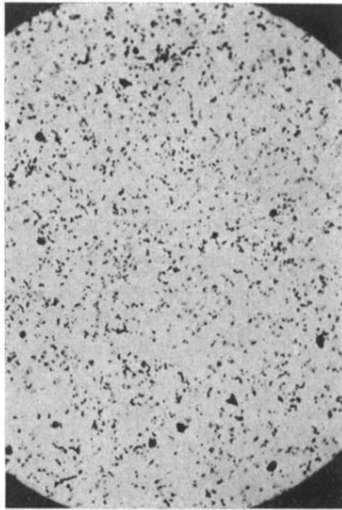


FIG. 5. Photomicrograph of Eastman NTB plate, exposed to 30-kv electrons, showing tracks of 4-5 grain length.